Using X-Ray As An Irradiation Source For Direct ESR Dating of Fossil Teeth

Wenjing Yu (Wenjing.Yu@latrobe.edu.au)
La Trobe University
A.I.R. Herries
La Trobe University
R. Joannes-Boyau
Southern Cross University

Research Article

Keywords: Electron spin resonance dating, dosimetry, fossil teeth, gamma irradiation, X-ray irradiation,

Posted Date: November 15th, 2021

DOI: https://doi.org/10.21203/rs.3.rs-1062274/v1

Version of Record: A version of this preprint was published at Quaternary Geochronology on July 16th, 2022. See the published version at https://doi.org/10.1016/j.quageo.2022.101372.

Abstract

In this paper we have tested the potential application of X-rays as an irradiation source in Electron Spin Resonance dating of tooth enamel. Both modern and fossil samples were used to assess the feasibility of dose estimations using this alternative irradiator. Equivalent doses obtained with gamma-rays on fossil powder enamel was frequently less than the doses obtained on fragments using only X-rays. It is believed that a combination of NOCORs (non-orientated CO_2^- radicals) and local internal dose discrepancy may be the origin of the difference. Here, we show that testing penetration attenuation for each individual irradiation source is required to accurately estimate the maximum enamel thickness and produce reliable protocols. The use of a known laboratory additive dose allows the calculation of an absorption equivalent coefficient between gamma-rays and X-rays. We conclude that X-rays are an alternative irradiation source for ESR dating protocols, however, limitations remain in particular with alpha efficiency.

1. Introduction

Electron Spin Resonance dating (ESR) is a trapped charge dating method that allows the dating of a wide variety of fossil and archaeological deposits across many different depositional settings and time periods[1–8] In South Africa, the low background cosmogenic dose makes it an ideal environment for ESR dating and this has allowed the dating of deposits at least as far back as ~2.61 Ma[1,4]. It has also been a crucial dating method for dating open air sites in the region where other methods were traditionally not applicable[9,10].However, more recently it is also used in conjunction with other methods such as luminescence and uranium-thorium dating on a timescale back to ~600 ka[2,11]; or uranium-lead dating and palaeomagnetism back to 2.6 Ma[4,5,12]. Critical to reliable ESR age estimates is the establishment of the archaeological dose of fossil teeth, which has been historically conducted using calibrated gamma sources [13–16]. However, access to such instruments has become a real issue for geochronologists due to changes in the global political environment, terrorist threats, and the intensification of general security concerns. Moreover, the inability to cross international, or even state boarders during a global pandemic such as COVID-19 has limited access to such gamma sources. These aforementioned reasons have impacted ESR dating of fossils, forcing researchers to come up with innovative protocols for dose recovery[17–21]. X-ray sources are easy to access, even in regional areas. Furthermore, the similar energy level and electromagnetic properties of X-rays compared to gamma rays make it an obvious choice, if it can be shown that the impact on enamel is identical for ESR dating purposes.

X-ray irradiation sources have been successfully used in luminescence dating [22–24] but there have been very few applications in ESR dating [20,25]. X-ray irradiation triggers an ESR signal on the enamel surface of exposed samples, inducing a reproducible gradient of irradiation impact[26,27]. However, the main hurdle for using X-ray sources is calibration as it appears to be a much more complex task than when using gamma rays due to the nature of the signal[8,12]. Gamma emission is mono-energetic, while X-ray emissions have a broader spectrum, with high to low energy photons, which greatly complicates

calibration of the source. Another problem is that the ionisation difference between X-rays and gamma rays is significant. When assuming an identical ionisation efficiency, the calculated ages with X-rays becomes implausibly young [20].

The aim of this study is to establish whether X-ray sources can be used as a replacement of gamma irradiation for the dose response curve (DRC), and accurate estimation of the dose equivalent (D_e). While, Grün *et al.* [20] looked into the fundamental differences and effect of X-rays and gamma rays to ESR samples, our approach was to simply establish an accurate gamma-ray/x-ray absorption coefficient. Thus, instead of using alanine, we have conducted our calibration and experiments directly on dental tissues to conduct our calibration and experiments.

To test this potential applicability, we have undertaken a range of experiments (i) an assessment of X-ray irradiation homogeneity; (ii) a comparison of enamel and alanine ionisation efficiency; (iii) enamel dose recovery by X-ray irradiation of modern samples with known gamma dose; (iv) establishing the discrepancy between gamma-ray and X-ray irradiation dose recovery on fossil samples.

2. Material And Methods

2.1 Sample Preparation

A series of modern and fossil primate (both human and non-human) and bovid teeth were prepared as described below for each irradiation experiment (Table 1 and Fig.1). X-ray irradiation sources were calibrated before the experiments. To characterise the X-ray sources and impact, three experimental settings (i, ii, iii) were tested on modern samples; while the last experiment (iv) used fossil enamel.

X-ray dose calibration to gamma: One modern human molar tooth (MH, provided by one of the authors) and a modern goat tooth (MG) recovered from a recently deceased animal were prepared. Two fragments of enamel were separated from each tooth (MH1, MH2, MG1 and MG2) and were cleaned of dentine and tartar. MH1 and MH2 were irradiated with gamma-rays for an equivalent dose of 50Gy and 400Gy, while MG1 and MG2 are given an equivalent doe of 200Gy and 800Gy respectively. For each enamel fragment a dose response curve (DRC) was calculated using an X-ray source, with the irradiation dose steps of 60s, 120s, 300s, 600s, 1800s, 3600s, 7200s 14400s and 66000s.

Characterisation of X-ray source and impact: A modern molar (A) was collected from a recently deceased bovid skull. Five long strips of enamel (2 to 3cm long by 4mm width) were extracted from the teeth using a diamond saw (tartar and dentine were removed from the surface of the enamel). One of the enamel strips (A1) was cut into seven equal aliquots (P1 to P7) and the other four strips (A2-A5) were sent to the Australian Nuclear Science and Technology Organisation (ANSTO) gamma irradiation facilities (Fig.1A).

(i) Six of the seven aliquots (P1 to P6) from A1 were irradiated for 600s using the X-ray source to evaluate X-ray penetration. While keeping the same surface area and prior to irradiation, the enamel aliquots were grounded to a specific thickness of: P1=650µm, P2=750µm, P3=1450µm, P4=1100µm, P5=1120µm and

P6=1230µm (±25µm). The first three aliquots (P1 to P3) were irradiated individually, while the later three aliquots (P4 to P6) were stacked together and irradiated as a single block. P1-P6 were then measured separately by ESR spectrometry (Fig. 1A).

(ii) The other enamel aliquot (P7) from the same strip (A1) was compared to an alanine pellet for X-ray ionisation efficiency (Fig. 1A). Both the alanine pellet and enamel aliquot were irradiated with X-ray successively for 60s, 120s, 300s, 600s, 1800s, 3600s and 7200s.

(iii)*:* The remaining four enamel strips (A2-A5) were sent to ANSTO to be irradiated by a gamma irradiation (see below for details), with each strip A2, A3, A4 and A5 receiving a specific dose of 50Gy, 200Gy, 400Gy and 800Gy respectively. From each strip, three aliquots were cut for the X-ray dose recovery procedure, with the following dose steps: 60s, 120s, 300s, 600s, 1800s, 3600s, 7200s 14400s and 66000s (Fig.1A).

Fossil Sample: (iv) A fossil bovid molar (B) was used to investigate the discrepancy between gamma and X-ray irradiation of dose recovery on fossil samples. Two adjacent fragments (B1&B2) were cut from the fossil tooth avoiding areas showing obvious diagenetic alteration, and cleaned from dentine and tartar using a diamond saw. One fragment (B1) was crushed into powder and separated into aliquots for gamma irradiation, while the other was kept for X-ray irradiation. The powder sample received gamma irradiation steps of 50Gy, 100Gy, 250Gy, 600Gy, 1200Gy, 2400Gy, 4000Gy, 8000Gy, 11000Gy and 17000Gy, while the intact fragment (B2) was given X-ray irradiation steps of 17Gy, 71Gy, 201Gy, 335Gy, 672Gy, 1352Gy, 2735Gy, 5398Gy and 11645Gy (Fig.1B).

Enamel fragments were extracted from three distinct non-human primate fossil teeth from China. For each tooth one small fragment was kept intact for the X-ray irradiation protocol, while the rest of the enamel was powdered and separated into 6 aliquots before receiving a gamma irradiation dose of 52.8, 203.5, 507.1, 1060, 2870 and 7820 Gy respectively.

2.2 Sample irradiation settings

Gamma irradiation of all the modern samples, as well as the three non-human primate fossil samples were performed at ANSTO on a Gamma cell 220 (cobalt-60) with a dose rate 23.8 Gy/min. Gamma irradiation for the powdered bovid fossil sample was performed at the CENIEH in Spain using a Gammacell-1000 instrument, encompassing a 137Cs gamma source with a dose rate of 7.27+0.06 Gy/min. The error in the gamma dose comes from both the decay calculation and the time precision at which the shutter shields the source, and the gamma dose error is set as 2%. X-ray irradiations were performed at Southern Cross University (SCU) on a Freiberg X-ray irradiation chamber, which contains a Varian VF50, with irradiation parameters of 40KV voltage and 0.5mA current. The samples were mounted onto a Teflon sample holder, which exposed the fragment directly to the X-ray source with ~200 microns Aluminum shielding (Fig. 2).

2.3 ESR spectrometer

ESR measurements at SCU were performed on a Freiberg Miniscope MS5000 (Fig. 2) at 1G modulation amplitude, 2mW power, 100G sweep, and 100KHz modulation frequency. All ESR intensities were measured for T1-B2 peak to peak over a z-configuration only (for more details see Joannes-Boyau 2013). All dose response curves (DRC) and equivalent dose (*De*) were calculated using the McDoseE 2.0 program from Joannes-Boyau *et al.*[29] with a single saturated exponential (SSE) fitting following recommendation from Duval *et al.* [30], Duval [31], and Duval and Grün[32].

3. Results And Discussion

3.1 X-ray dose calibration to gamma

For each modern human and bovid fragment (MH1&2 and MG1&2), we obtained a linear relationship between the X-ray calculated dose equivalent (D_e) in seconds and the gamma irradiation known dose given to the samples (Fig. 3). The dose absorbed by the enamel fragment d_a (Gy) can then be calculated using the following equation:

$$d_a = aTD \qquad (1)$$

with *a* the absorption equivalent coefficient, *D* the dose rate (Gy.s^{-1}) and *T* the irradiation time (s).

The following is an example for MH1 (gamma irradiation of 50Gy):

$$a = {}^{d_a}/_{TD} = \frac{50}{438 \times 4.255} = 0.0268 \qquad (2)$$

Table 2 calculates the absorption equivalent coefficient values of 0.0268 (2), 0.0286, 0.0276 and 0.0276 for MH1, MG1, MH2, and MG2 respectively. We obtained an average value of *a* = 0.0277 ± 0.001. Using this value, we obtained 51.6±2.6Gy, 193.5±9.6 Gy, 400.1±19.5Gy and 801.7±42.1 Gy for the gamma dose equivalent of MH1, MG1, MH2, and MG2 respectively. The dose obtained is close to the expected gamma-dose since it is used to calculate the *a* coefficient.

3.2 Assessment of X-ray irradiation homogeneity

This experiment was designed to look into the X-ray penetration depth for enamel density at 40KV. The aim is to validate the maximum thickness of samples that can be used for dose recovery using X-ray irradiation if a control gamma dose is given to the sample. Fig.4A shows that the ESR intensity appears to remain constant for fragments thinner than 1500µm, and then decreases rapidly. The X-ray penetration depth has shown us that as long as the enamel fragment is thinner than 1500µm, the X-ray influence should be homogenous (respective to our irradiation setting, e.g. voltage and intensity). The exact

penetration depth could vary for different samples depending on the enamel density, as well as from the X-ray gun efficiency. However, it is estimated that the enamel density discrepancy between bovid and primate teeth would be unlikely to induce a significant variation in the X-ray penetration depth. It is currently unknown whether significant diagenetic processes impacting enamel density, could drastically change penetration. However, the variation in thickness would have to be significant to impact ESR dating beyond the existing and rather large uncertainties.

3.3 *Enamel/Alanine ionisation efficiency*

It has previously been reported that X-ray alanine ionisation was different to enamel ionisation due to the large energetic spectrum of emission and because of the density difference between the two materials [20,33]. Our results have shown a similar outcome, with the alanine and enamel ESR signal exhibiting different ionisation efficiencies (Fig.4B). The ESR intensities discrepancy between alanine and enamel varies with irradiation steps, as illustrated by the enamel/alanine intensity ratio (E/A) in Fig. 4B. At first the E/A ratio is >1, but after only 120s (equivalent of about ~75Gy) the alanine sample becomes increasingly more sensitive to X-rays than the enamel, and the E/A ratio becomes <1. The growth curve of enamel saturates much faster than the alanine response. This induces the E/A ratio to decrease exponentially, reaching an asymptote comparable to the inverse of the density ratio E/A (around 0.5). The fact that alanine and enamel have very different ionization efficiencies is certainly of concern. However, two fundamental differences between alanine and enamel could contribute to the results. Firstly, the alanine pellets are much thicker than the enamel layer (300% more). Secondly, the surface to volume ratio of the enamel is greater than the alanine sample, making it more sensitive to small doses and potentially more rapid saturation. Historically, alanine pellets have been used for source calibration and subsequently for ESR dosimetry. Since, the two materials behave differently with X-ray irradiation, we argue the calibration of the source using alanine pellets is not transferable to enamel fragments because of the ionizing discrepancy.

3.4 Enamel dose recovery of known gamma dose

Results for modern fragments (A2-A5) are summarized in Table 3A. The absorption equivalent coefficient average value (*a=0.0277± 0.001)* was used to calculate each irradiation time into irradiation dose in Gy. Results show that the estimated doses are offset by 5% for 50Gy, 7% for 200Gy, 5% for 400Gy and 5% for 800Gy, without considering the associated error, which falls into the general ESR uncertainty. All equivalent dose (D_e) estimates for modern samples were statistically indistinguishable with the respective gamma dose received originally.

For all modern samples, X-ray irradiation protocols have proven to be a precise (within error) alternative source for the calculation of the equivalent gamma. The results also suggest that the discrepancy between the dose equivalent obtained compare to the gamma dose received by the sample is not influenced by the intensity of the dose itself. For example, the lowest dose (50Gy) and the largest dose (800Gy) show similar deviation over the dose equivalent results. One must keep in mind that the main

limitation of this experiment remains that different aliquots divided from the same samples were used for the absorption equivalent coefficient and the dose recovery. Ideally, a range of other modern samples from separate teeth should be tested in the future to further validated the accuracy of DRC calculation using X-ray source.

3.5 The discrepancy between X-ray and Gamma-ray for fossil samples

Unlike modern samples, fossil dose equivalents estimated by X-ray irradiation are significantly higher (~ 20%) than the one obtained with gamma (Fig. 5A, Table 3B). All have larger discrepancies between D_e than the associated errors, making each paired result statistically distinct. The discrepancy obtained with fossil samples could possibly be linked to enamel modification during burial and fossilization.

Fig.5B further compares the DRC of fossil fragments using gamma irradiation versus X-ray irradiation. The ESR intensities are significantly higher for fossil fragments irradiated by gamma than when using an X-ray source. A potential explanation for this effect could be the creation of unstable non-orientated CO_2^- radicals (NOCORs) by gamma irradiation [21,34], a known leading cause for D_e underestimation in fossil teeth[35]. However, X-ray irradiation has been proven to marginally create unstable radicals [20]. An average value of ~20% of NOCORS to the total D_e estimation has generally been observed in fossil teeth [28,35,36]. If accurate, X-ray irradiation would not only offer a more convenient alternative to gamma irradiation but also a more accurate dose reconstruction protocol. A previous study[8], has already established the lesser impact of X-ray irradiation in the creation of unstable radicals. However, further research on the behaviour of radicals and creation under X-ray is necessary. Another explanation for these differences could be that the initial doses between the enamel used for the powder and the fragment measurements from the same fossil tooth could somehow be different enough to induce such differences. While possible, this explanation is highly unlikely since the offset between X-ray and gamma-ray calculated D_e appears to range around 20%, and would be hard to explain on four distinct samples.

Conclusion

X-ray sources remains a very promising alternative to gamma irradiator for ESR dating of fossil teeth. However, additional work is needed to better understand the impact of X-rays on radical formation and to obtain more accurate DRC calculations. Our results also establish that X-ray attenuation on enamel fragments is minimal when an enamel thickness is inferior to 1500µm for our specific settings, offering homogenous irradiation throughout the sample. Unfortunately, as each source is different, the protocol needs to be validated for specific settings and parameters.

Similar to previous studies, our results have shown that alanine and enamel have different ionization efficiency, making the use of alanine pellets unreliable for X-ray source calibration. It is therefore recommended that each X-ray source be calibrated using the same datable material (e.g. quartz for quartz, enamel for enamel, etc…).

X-ray protocols on enamel fragments using an absorption equivalent coefficient obtained with known gamma dose appears to offer reliable dose equivalent estimates on modern samples. Fossil samples however exhibit significant discrepancy that we believe should be attributed to the difference in unstable radicals' concentration generated by the various irradiation sources. The use of X-rays as an irradiation source could potentially bring ESR dating to the next stage where the irradiation source is safer, more convenient, as well as improving dating efficacy and accuracy.

Declarations

Acknowledgement

We would like to thank ANSTO facility for providing access to the irradiation facility and Southern Cross University generous contribution towards the installation of the ESR spectrometer. We thank Dr Mathieu Duval for sharing gamma irradiated enamel powder data with us. This research was supported through; ARC discovery grants ARC DP140100919 to RJB and ARC DP170100056 to AIRH and RJB. It was also supported by Higher Degree Research fee waivers and living scholarships from La Trobe University and the La Trobe University Humanities and Social Science Internal Research Grant Scheme 2019-3-HDR-0012 to WY.

Author contributions statements

All authors (W. Yu, A.I.R. Herries and R. Joannes-Boyau) participated in the experimental design, figure preparation and manuscript writing.

Additional Information

The authors declare no competing interests.

References

1. Herries, A. I. & Shaw, J. Palaeomagnetic analysis of the Sterkfontein palaeocave deposits: Implications for the age of the hominin fossils and stone tool industries. *Journal of Human Evolution* **60**, 523–539 (2011).

2. Dirks, P. H. *et al.* The age of *Homo naledi* and associated sediments in the Rising Star Cave, South Africa. *eLife* **6**, e24231 (2017).

3. Richter, D. *et al.* The age of the hominin fossils from Jebel Irhoud, Morocco, and the origins of the Middle Stone Age. *Nature* **546**, 293–296 (2017).

4. Herries, A. I. R. *et al.* Geoarchaeological and 3D visualisation approaches for contextualising in-situ fossil bearing palaeokarst in South Africa: A case study from the ~2.61 Ma Drimolen Makondo. *Quaternary International* **483**, 90–110 (2018).

5. Herries, A. I. R. *et al.* Contemporaneity of *Australopithecus, Paranthropus*, and early *Homo erectus* in South Africa. *Science* **368**, eaaw7293 (2020).

6. Han, F., Shao, Q., Bahain, J.-J., Sun, X. & Yin, G. Coupled ESR and U-series dating of Middle Pleistocene hominin site Bailongdong cave, China. *Quaternary Geochronology* **49**, 291–296 (2019).

7. Withnell, C. B., Joannes-Boyau, R. & Bell, C. J. A reassessment of the age of the fauna from Cumberland Bone Cave, Maryland, (middle Pleistocene) using coupled U-series and electron spin resonance dating (ESR). *Quaternary Research* **97**, 187–198 (2020).

8. Rizal, Y. *et al.* Last appearance of *Homo erectus* at Ngandong, Java, 117,000–108,000 years ago. *Nature* **577**, 381–385 (2020).

9. Grün, R. *et al.* Direct dating of Florisbad hominid. *Nature* **382**, 500–501 (1996).

10. Porat, N. *et al.* New radiometric ages for the Fauresmith industry from Kathu Pan, southern Africa: implications for the Earlier to Middle Stone Age transition. *Journal of Archaeological Science* **37**, 269–283 (2010).

11. Pickering, R. *et al.* Stratigraphy, U-Th chronology, and paleoenvironments at Gladysvale Cave: insights into the climatic control of South African hominin-bearing cave deposits. *Journal of Human Evolution* **53**, 602–619 (2007).

12. Herries, A. I. R. & Adams, J. W. Clarifying the context, dating and age range of the Gondolin hominins and *Paranthropus* in South Africa. *Journal of Human Evolution* **65**, 676–681 (2013).

13. Schwarcz, H. P. ESR studies of tooth enamel. *Nuclear Tracks and Radiation Measurements (1982)* **10**, 865–867 (1985).

14. Lee, H.-K., Rink, W. J. & Schwarcz, H. P. Comparison of ESR signal dose-responses in modern and fossil tooth enamels. *Radiation measurements* **27**, 405–411 (1997).

15. Grün, R. & Stringer, C. Tabun revisited: revised ESR chronology and new ESR and U-series analyses of dental material from Tabun C1. *Journal of human Evolution* **39**, 601–612 (2000).

16. Bahain, J.-J. *et al.* ESR chronology of the Somme River Terrace system and first human settlements in Northern France. *Quaternary Geochronology* **2**, 356–362 (2007).

17. Joannes-Boyau, R. & Grün, R. Decomposition of beta-ray induced ESR spectra of fossil tooth enamel. *Radiation Physics and Chemistry* **80**, 335–342 (2011).

18. Joannes-Boyau, R., Bodin, T. & Grün, R. Decomposition of the angular ESR spectra of fossil tooth enamel fragments. *Radiation Measurements* **45**, 887–898 (2010).

19. Joannes-Boyau, R., Grün, R. & Bodin, T. Decomposition of the laboratory gamma irradiation component of angular ESR spectra of fossil tooth enamel fragments. *Applied Radiation and Isotopes* **68**, 1798–1808 (2010).

20. Grün, R., Mahat, R. & Joannes-Boyau, R. Ionization efficiencies of alanine dosimeters and tooth enamel irradiated by gamma and X-ray sources. *Radiation Measurements* **47**, 665–668 (2012).

21. Joannes-Boyau, R. & Grün, R. Thermal behavior of orientated and non-orientated CO2− radicals in tooth enamel. *Radiation Measurements* **44**, 505–511 (2009).

22. Andersen, C. E., Bøtter-Jensen, L. & Murray, A. S. A mini X-ray generator as an alternative to a 90Sr/90Y beta source in luminescence dating. *Radiation Measurements* **37**, 557–561 (2003).

23. Yawata, T. & Hashimoto, T. Availability of a small X-ray tube combined with Al-absorber as a new irradiator for luminescence researches. *Radioisotopes (Tokyo)* **53**, 207–212 (2004).

24. Thomsen, K. J., Bøtter-Jensen, L., Denby, P. M. & Murray, A. S. Luminescence response to irradiation using mini X-ray generators. *Nuclear Instruments and Methods in Physics Research Section B: Beam Interactions with Materials and Atoms* **252**, 267–275 (2006).

25. Tsukamoto, S., Toyoda, S., Tani, A. & Oppermann, F. Single aliquot regenerative dose method for ESR dating using X-ray irradiation and preheat. *Radiation Measurements* **81**, 9–15 (2015).

26. Ikeya, M. A model of linear uranium accumulation for ESR age of Heidelberg (Mauer) and Tautavel bones. *Japanese Journal of Applied Physics* **21**, L690 (1982).

27. Oppermann, F. & Tsukamoto, S. A portable system of X-ray irradiation and heating for electron spin resonance (ESR) dating. *Ancient TL* **33**, 11–15 (2015).

28. Joannes-Boyau, R. Detailed protocol for an accurate non-destructive direct dating of tooth enamel fragment using Electron Spin Resonance. *Geochron* **40**, 322–333 (2013).

29. Joannes-Boyau, R., Duval, M. & Bodin, T. MCDoseE 2.0 A new Markov Chain Monte Carlo program for ESR dose response curve fitting and dose evaluation. *Quaternary Geochronology* **44**, 13–22 (2018).

30. Duval, M., Grün, R., Falgueres, C., Bahain, J.-J. & Dolo, J.-M. ESR dating of Lower Pleistocene fossil teeth: limits of the single saturating exponential (SSE) function for the equivalent dose determination. *Radiation Measurements* **44**, 477–482 (2009).

31. Duval, M. Evaluating the accuracy of ESR dose determination of pseudo-Early Pleistocene fossil tooth enamel samples using dose recovery tests. *Radiation Measurements* **79**, 24–32 (2015).

32. Duval, M. & Grün, R. Are published ESR dose assessments on fossil tooth enamel reliable? *Quaternary Geochronology* **31**, 19–27 (2016).

33. Iwasaki, M. *et al.* Energy Dependence of the CO3 3-Signal Intensity in ESR Dosimetry of Human Tooth Enamel. *Radioisotopes* **40**, 421–424 (1991).

34. Grün, R., Joannes-Boyau, R. & Stringer, C. Two types of CO2− radicals threaten the fundamentals of ESR dating of tooth enamel. *Quaternary Geochronology* **3**, 150–172 (2008).

35. Joannes-Boyau, R. & Grün, R. A comprehensive model for CO2− radicals in fossil tooth enamel: implications for ESR dating. *Quaternary Geochronology* **6**, 82–97 (2011).

36. Joannes-Boyau, R. & Grün, R. Decomposition of UV induced ESR spectra in modern and fossil dental enamel fragments. (2010).

Tables

Due to technical limitations, tables 1,2 and 3 are only available as a download in the Supplemental Files section.

Figures

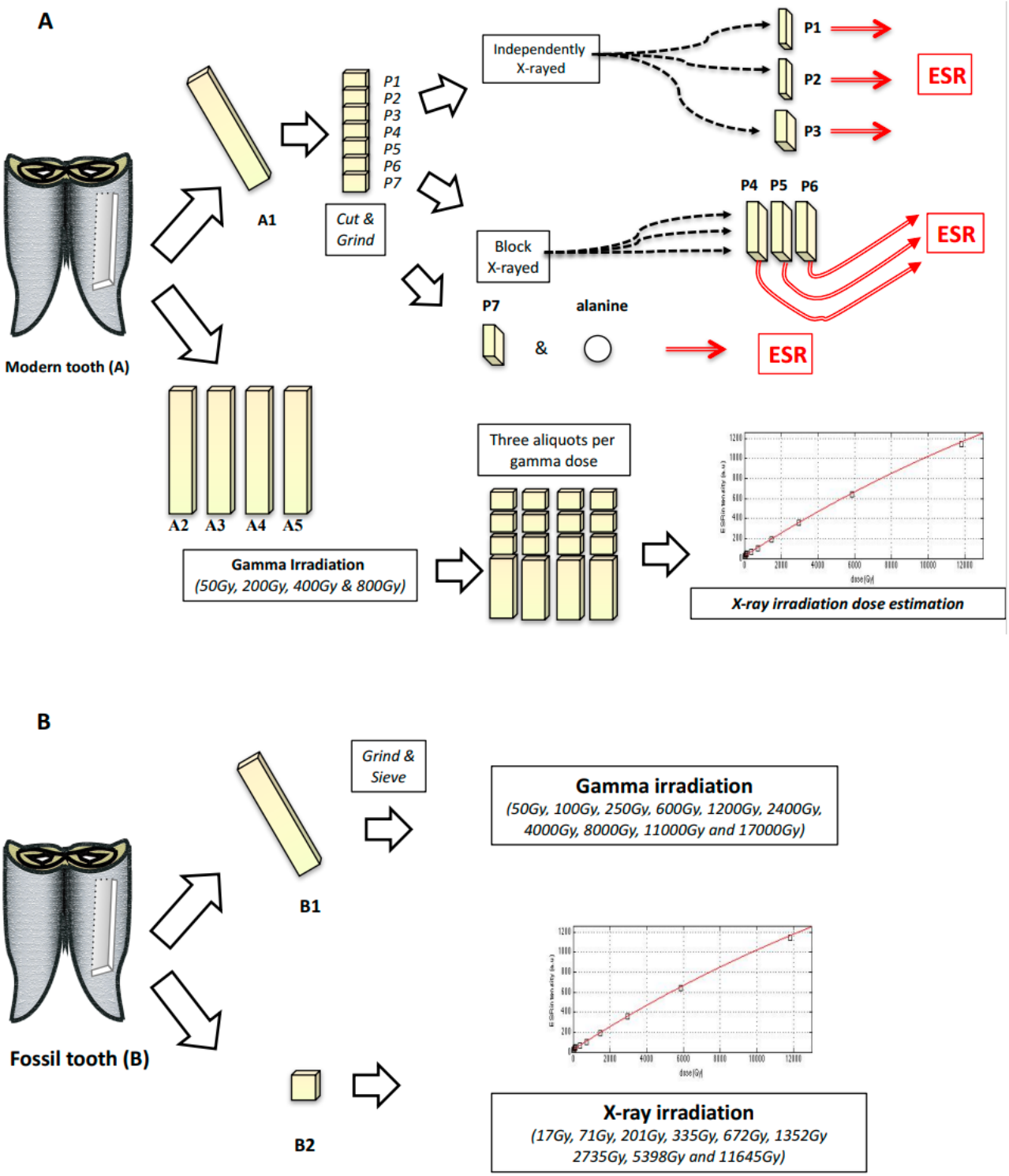

Figure 1

Material for the experimental settings. A) Experimental settings for X-ray depth assessment (A1; strips P1-P6), X-ray ionisation efficiency (A1; strip P7 & alanine), and enamel dose recovery of known gamma dose (A2-A5) on a modern bovid tooth; B) Experimental settings for investigating the discrepancy between gamma (B1) and X-ray irradiation (B2) of dose recovery on a fossil bovid tooth.

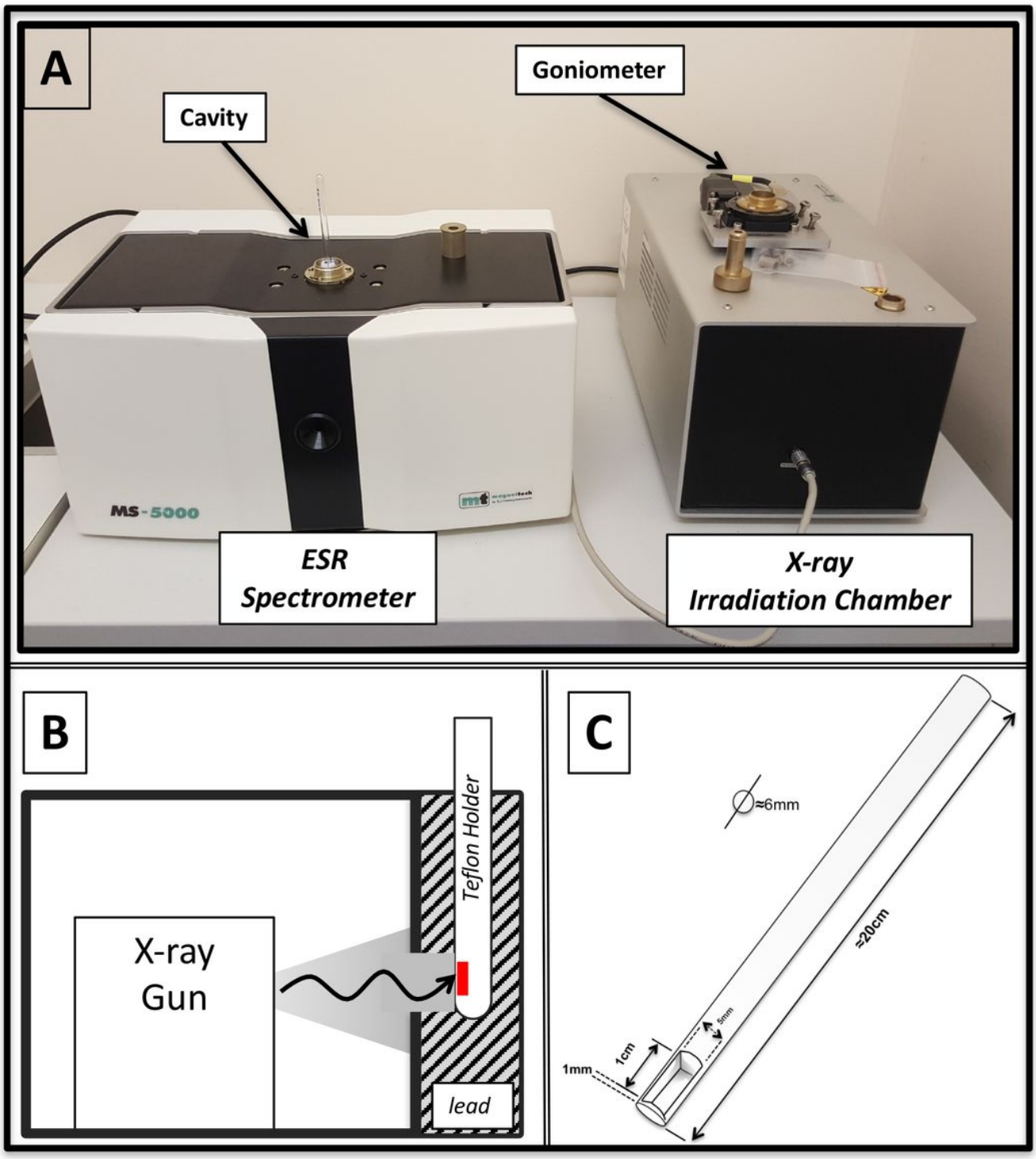

Figure 2

Southern Cross University ESR spectrometer settings. A) photo of the ESR spectrometer on the left and X-ray irradiation on the right; B) Simplified drawing of the inside of the X-ray irradiation chamber; C) Teflon holder for irradiating enamel fragments.

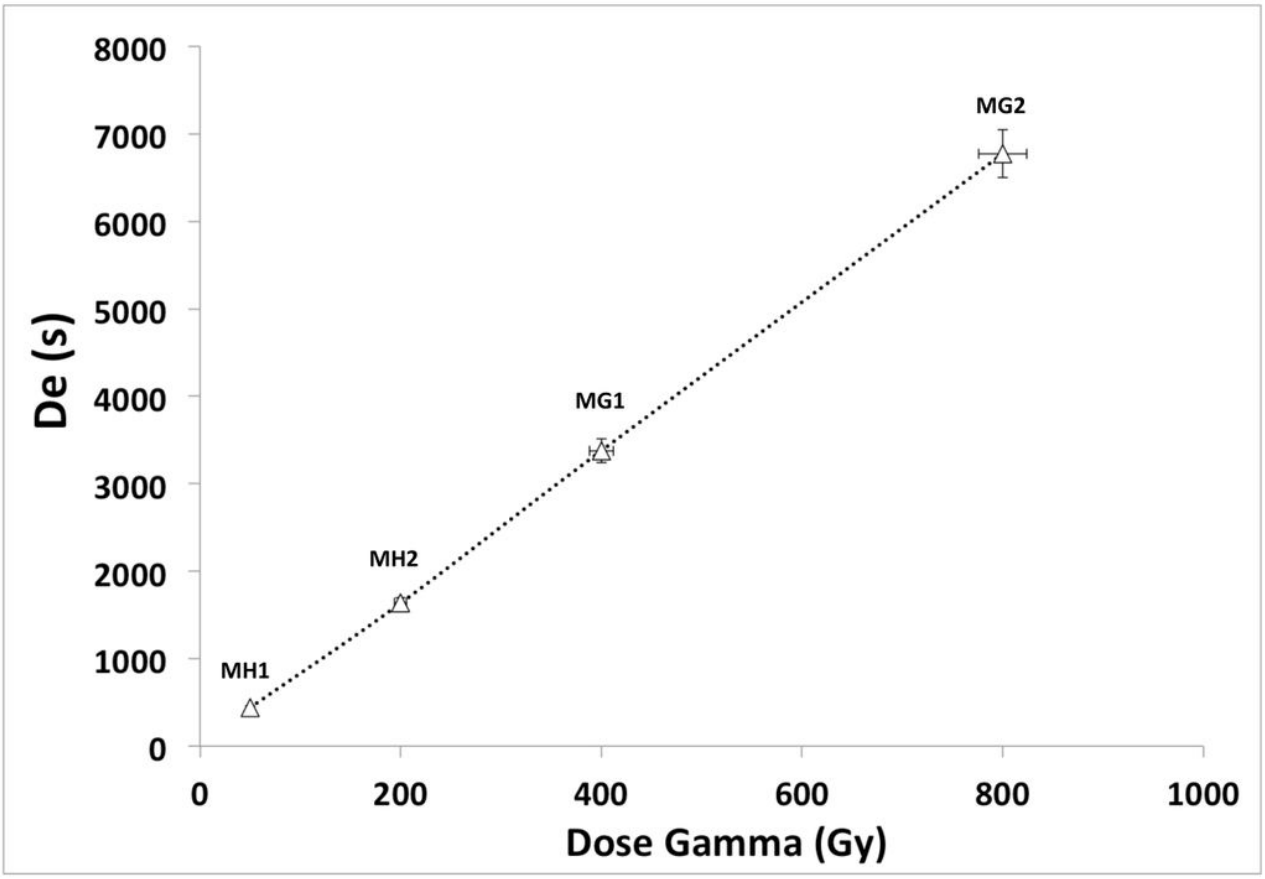

Figure 3

Relationship between the Dose equivalent obtain using X-ray irradiation and the known gamma dose given to the samples.

A

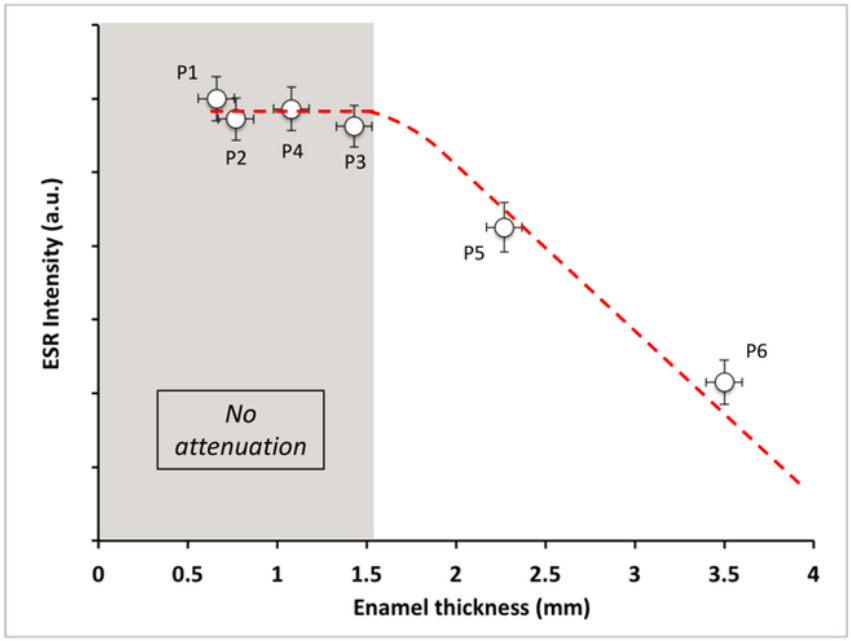

B

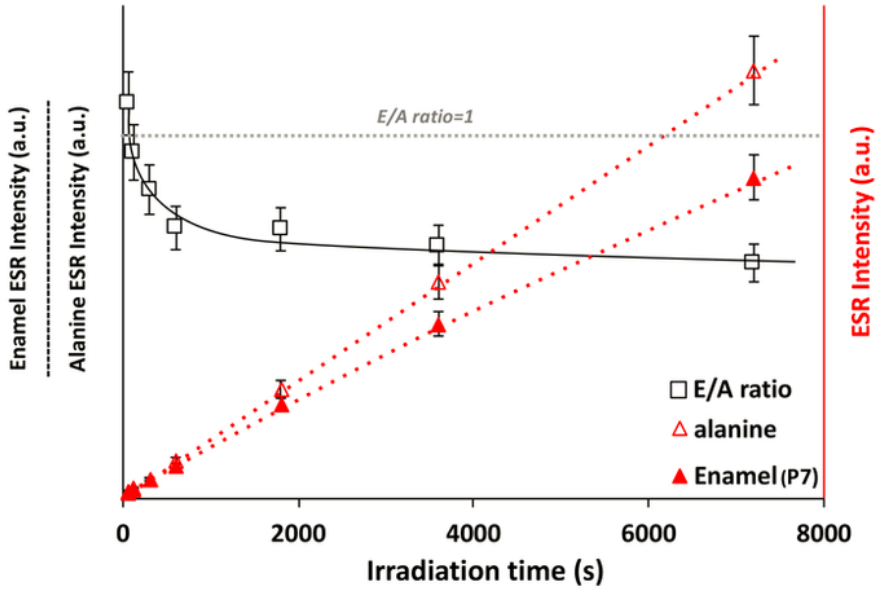

Figure 4

A) X-ray penetration depth, using the ESR intensity as a function of the enamel thickness. Enamel strip P1-P3 were independently X-rayed while P4-P6 were block X-rayed. Of note that the dotted curve is a simulated curve to help the reader visualizing the X-ray attenuation pattern, it does not correspond to a real trend. B) Comparison of the ionization efficiency between tooth enamel (P7) and alanine pellets.

Black squares represent the enamel ESR intensity/alanine ESR intensity ratio. Red curves represent the ESR intensity of each samples; the enamel fragment appears to saturate more than the alanine.

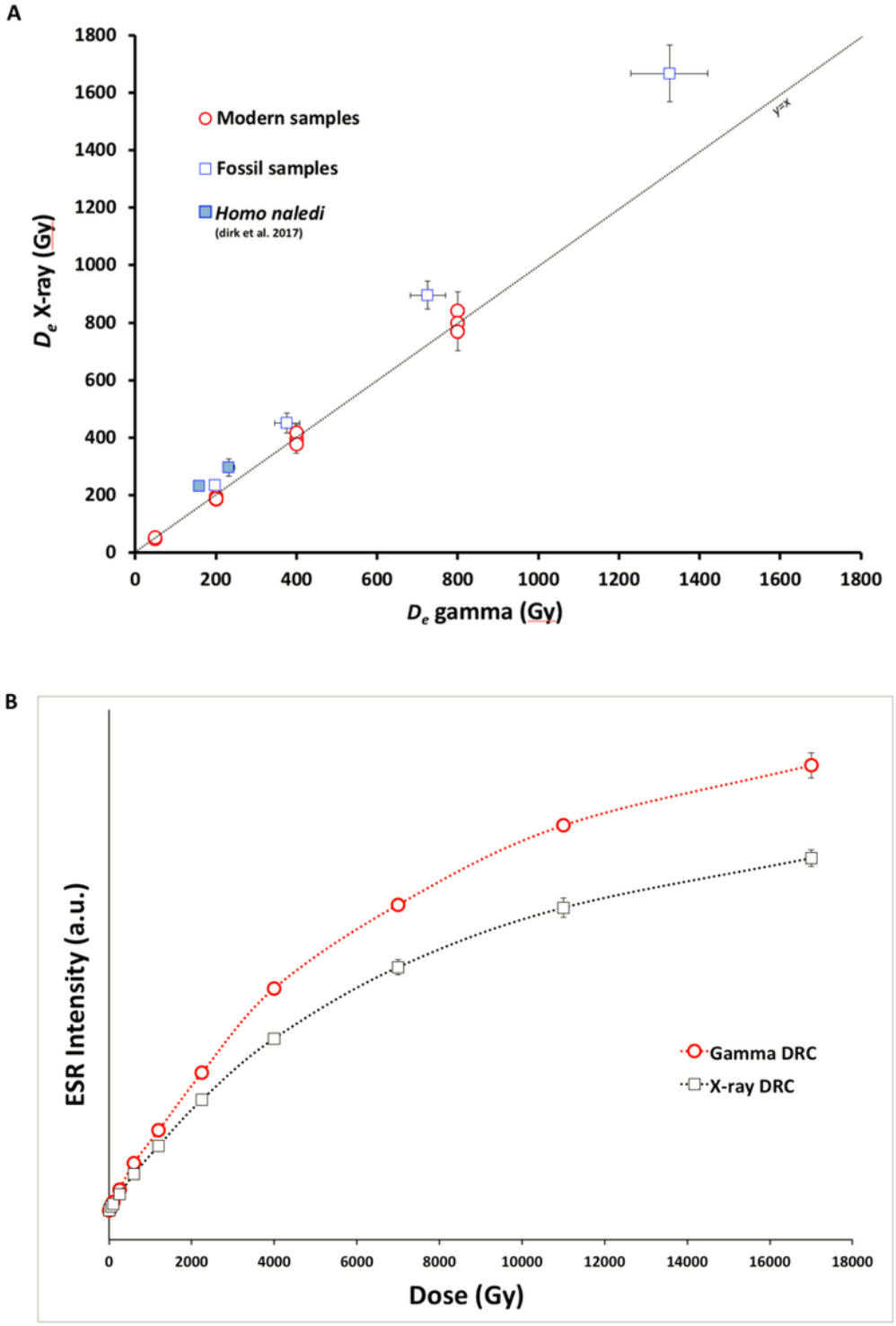

Figure 5

A)Comparison between De obtained using X-ray and gamma irradiations, modern sample (red circle), fossil samples (empty blue square) and Homo naledi samples data (full blue square, adapted from Dirks et al.2); B)Comparison of the dose response curves obtained using gamma irradiation (red circle) versus

X-ray irradiation (black square) of fossil samples. ESR intensities were normalised to the Natural dose (irradiation t=0s)

Supplementary Files

This is a list of supplementary files associated with this preprint. Click to download.

- TablesXrayFinal.pptx